

## Domain wall network as QCD vacuum: confinement, chiral symmetry, hadronization

---

**Sergei N. Nedelko**<sup>\*†</sup>

*Bogoliubov Laboratory of Theoretical Physics, Joint Institute for Nuclear Research*

*E-mail: nedelko@theor.jinr.ru*

**Vladimir E. Voronin**

*Bogoliubov Laboratory of Theoretical Physics, Joint Institute for Nuclear Research*

*E-mail: voronin@theor.jinr.ru*

We give a short review of the motivation and results of the approach to QCD vacuum as a medium describable in terms of statistical ensemble of almost everywhere covariantly constant Abelian self-dual and anti-self-dual gluon fields which also can be seen as an ensemble of domain wall networks. An overview of the quark confinement, chiral symmetry realization and hadronization formalism based on the ensemble of domain structured gluon fields is given. The domain walls separate the regions with Abelian self-dual and anti-self-dual fields. The network of the domain wall defects is introduced as a combination of multiplicative and additive superposition of kinks. The character of the spectrum and eigenmodes of elementary color-charged fluctuations and colorless collective meson modes in the presence of the domain wall network is discussed. Conditions for the formation of a stable thick domain wall junction (the chromomagnetic trap) during heavy ion collisions and the spectrum of color charged quasiparticles inside the trap are discussed. The critical size  $R_c$  of the trap stable against gluon tachyonic modes is related to the value of gluon condensate  $\langle g^2 F^2 \rangle$ . The growth of large lumps of merged chromomagnetic traps and the concept of the confinement-deconfinement transition in terms of the ensemble of domain wall networks are outlined. New results for radial excitations of light, heavy-light mesons and heavy quarkonia are presented.

*XXII International Baldin Seminar on High Energy Physics Problems,*

*15-20 September 2014*

*JINR, Dubna, Russia*

---

<sup>\*</sup>Speaker.

<sup>†</sup>We are grateful to the organizing committee for the opportunity to give an extended review talk.

## 1. Overview of the approach

As in other quantum systems with infinitely many degrees of freedom, the global minima of the QCD effective action define its vacuum structure. A nontrivial global minimum corresponds to a gauge field with the strength not vanishing at space-time infinity and, hence, extensive classical action proportional to the four dimensional space-time volume of the system. The identification of global minima in different regimes (high energy density, high baryon density, strong external electromagnetic fields) is important for understanding the phase transformations in hadronic matter. Degenerate global minima related by discrete symmetry transformations like CP, Weyl symmetry in the root space of  $su(N_c)$ , center symmetry, is a reason to look for field configurations interpolating between them. First of all, these are domain wall configurations, but also lower dimensional topological defects at the domain wall junctions.

A variety of essentially equivalent statements of the problem in the context of QCD can be found in [2, 3, 4, 5, 6] and [7], in particular. In the Euclidean formulation, the statement of the problem starts with the very basic symbol of the functional integral

$$Z = N \int_{\mathcal{F}} DA \exp\{-S[A]\},$$

where the functional space  $\mathcal{F}$  is subject to the condition

$$\mathcal{F} = \{A : \lim_{V \rightarrow \infty} \frac{1}{V} \int d^4x g^2 F_{\mu\nu}^a(x) F_{\mu\nu}^a(x) = B_{\text{vac}}^2\}. \quad (1.1)$$

The constant  $B_{\text{vac}}$  is not equal to zero in the general case, which is equivalent to nonzero gluon condensate  $\langle g^2 F^2 \rangle$ . The phenomenology of strong interactions has required nonzero gluon condensate, which suggests that it must be allowed in the QCD functional integral from the very beginning. Condition (1.1) singles out fields  $B_{\mu}^a$  with the strength which is non-zero almost everywhere in  $R^4$ . The homogeneous fields with the domain wall defects are the most natural gluon configurations which are homogeneous almost everywhere in  $R^4$  and satisfy condition (1.1).

Separation of the modes  $B_{\mu}^a$  responsible for gluon condensate and the local fluctuations  $Q_{\mu}^a$  in the background  $B_{\mu}^a$ , must be supplemented by the gauge fixing condition. The background gauge condition for fluctuations  $D(B)Q = 0$  is the most natural choice. Further steps include integration over the fluctuation fields  $Q$  resulting in the effective action for the long-range fields and identification of the minima of this effective action (for more details see [9] and [6, 7, 8]) which dominate over the integral in the limit  $V \rightarrow \infty$  and define the phase structure of the system. As soon as minima are identified, this setup defines a principal scheme for self-consistent identification of the class of gauge fields which almost everywhere in  $R^4$  coincide with the global minima of the quantum effective action. A treatment of these ‘‘vacuum fields’’ in the QCD functional integral

$$Z = N' \int_{\mathcal{B}} DB \int_{\Psi} D\psi D\bar{\psi} \int_{\mathcal{Q}} DQ \det[D(B)D(B+Q)] \delta[D(B)Q] \exp\{-S_{\text{QCD}}[B+Q, \psi, \bar{\psi}]\} \quad (1.2)$$

must be nonperturbative. The fields  $B_{\mu}^a \in \mathcal{B}$  are subject to condition (1.1) with the fixed vacuum value of the condensate  $B_{\text{vac}}^2$ . The condensate plays the role of the scale parameter of QCD to be

identified from the hadron phenomenology. The gluon  $Q$  and quark  $\psi$  fluctuations in the background of the vacuum fields can be seen as perturbations.

Many aspects of this general idea has been elaborated in the Copenhagen model of QCD vacuum [10, 11, 12, 13]. The starting point was the Savvidy's observation that the pure Yang-Mills one-loop effective action for the homogeneous chromomagnetic field indicated a minimum at the nonzero field strength [14, 15]. The Copenhagen vacuum is represented by the ensemble of domain structured gluon configurations - a network of domain wall defects in the constant chromomagnetic field. The inhomogeneities due to the domain walls remove tachyonic gluon mode inherent to the constant chromomagnetic field. Copenhagen vacuum gluon configurations were recognized as the color magnetic flux tube system [13] with the properties of quantum liquid. This approach turned out to be very fruitful as it triggered numerous applications varying from the physics of confinement in QCD to compact stars and early Universe. Particularly important result of Olesen was a proof of relevance of the randomness of the ensemble of chromomagnetic flux tubes to the area law for the spacial Wilson loop [16]. For the sake of further comparison we note here that any given configuration in the flux tube ensemble is characterized by  $\tilde{F}F \equiv 0$  (this is a pure chromomagnetic field),  $F^2 = 0$  at the boundary of the tube and  $F^2 \neq 0$  for the rest of space.

Another important benchmark was the analysis of general features of the quantum effective action in  $SU(2)$  gauge model given by Pagels and Tomboulis [3]. The most important for the context of our approach is the observation that condition (1.1) can lead to the vacuum fields behaving as a medium infinitely stiff to small gauge field fluctuations, that is seen as the absence of the wave solutions for the effective quantum equations of motion. This feature was interpreted as suggestive of confinement of color. Approximately at the same time an interplay between chiral symmetry breaking and strong CP violation was studied by Minkowski in the context of self-dual constant background field [2].

Strong argumentation in favour of the Abelian (anti-)self-dual homogeneous field as a candidate for the global minimum of the effective action originates from the papers [4, 5, 17, 18, 19, 20]. In particular, Leutwyler's analysis of all different types of the gauge fields with the constant strength has indicated that the gauge field is stable against small quantum fluctuations only if it is Abelian (anti)self-dual covariantly constant field. Other constant fields are unstable due to tachyonic gluon modes [4, 5]. Nonperturbative calculation of the effective potential within the functional renormalization group [19] supported the earlier one-loop results on existence of the nontrivial minimum of the effective action for the Abelian (anti-)self-dual field.

Leutwyler [21] noticed that the momentum representation of the translation invariant part of the propagator of the color charged field in the background of dual or anti-self-dual Abelian gauge field is entire analytical function and interpreted the absence of poles in propagator as color confinement. For example Euclidean propagator of the charged massless scalar field has the form

$$G(p^2) \sim \frac{1}{p^2} \left(1 - e^{-p^2/B_{\text{vac}}}\right). \quad (1.3)$$

The absence of pole in the propagator was treated as the absence of the particle interpretation of the charged field. On the other hand, for large Euclidean momentum  $p^2 \gg B_{\text{vac}}$  the propagator takes the standard form of a free massless one. Analytical properties of above propagator reflect the character of eigenmodes and the spectrum of the color charged field. The spectrum is purely

discrete and the eigenmodes have the character of bound state functions in all four directions. This was a novel point of view on the role of the background vacuum fields in the confinement mechanism. However just the absence of a single quark or anti-quark in the spectrum can not be considered as sufficient condition for confinement. The above given type of the color charged propagator seemed to have no obvious relation to the most peculiar feature of QCD - the Regge character of the physical spectrum of colorless hadrons. Usually Regge spectrum is related to the string picture of confinement [1]. Neither the homogeneous Abelian (anti-)self-dual field itself nor the propagator above had the clue to linear quark-antiquark potential. Nevertheless the analytic structure of this propagator and assumption about the randomness of this field gave an unexpected result.

The constant gauge vacuum fields bring too much order into the system and would mean violation of essentially all the symmetries of QCD. Randomness of the ensemble of the domain structured almost everywhere homogeneous Abelian (anti-)self-dual gluon fields has been taken into account implicitly in the model of hadronization developed in [22, 23] via averaging of the quark loops over the parameters of the background Abelian (anti-)self-dual fields. The nonlocal quark-meson vertices with the complete set of meson quantum numbers were determined in this model by the form of the color charged gluon propagator (1.3). The spectrum of mesons displayed the Regge character both with respect to total angular momentum (spin) and radial quantum number of the meson [22, 23]. Regge spectrum occurs due to the nonlocal Gaussian exponent terms in quark and gluon propagators akin to (1.3). The reason for confinement of a single quark and Regge spectrum of mesons turned out to be the same. Within this relativistic quantum field description the Regge spectrum of color neutral collective modes appeared as a "medium effect" as well as the suppression (confinement) of a color charged elementary modes.

However, besides this dynamical color charge confinement, a correct complete picture must include the limit of static quark-antiquark pair with the area law for the temporal Wilson loop. In order to explore this aspect an explicit construction of the random domain ensemble was suggested in paper [6], and the area law for the Wilson loop was demonstrated by the explicit calculation. Randomness of the ensemble (in line with [16]) and (anti-)self-duality of the fields are crucial for this result. For simplicity, the domains in  $R^4$  were taken to be spherical in this model.

The model of confinement, chiral symmetry breaking and hadronization based on the dominance of the random ensemble of gluon fields which are (anti-)self-dual Abelian almost everywhere demonstrated high overall phenomenological performance [6, 8, 23, 24]. It incorporated the majority of essential physics of confinement, chiral symmetry realization and hadronization from the single point of view. The model exhibits confinement of static (area law) and dynamical quarks (absence of poles in the propagators of color charged fields, discrete spectrum of the corresponding differential operator), spontaneous breakdown of the flavour chiral symmetry,  $U_A(1)$  symmetry is broken due to the axial anomaly, strong  $CP$  violation is absent in the model in line with the mechanism indicated by Minkowski [2] long time ago. With a minimal set of parameters (quark masses, gauge coupling constant, gluon condensate and mean domain size related to the topological susceptibility of pure YM) the model has demonstrated ability to give rather accurate results for meson masses from all different parts of the spectrum: light mesons including excited states, heavy-light mesons, heavy quarkonia). The decay constants and some form factors were also calculated within the model. New improved results for the spectrum of radial excitations of mesons are presented in

some detail in the last section.

These phenomenological results required more detailed study of the formation of the random ensemble under consideration, the domain wall formation in particular. Within the Ginzburg-Landau approach to the quantum effective action [6, 18, 9] the relevant domain wall was described by the sine-Gordon kink for the angle between chromomagnetic and chromoelectric components of the gluon field. This kink configuration can be seen as plain domain wall separating the regions with self-dual and anti-self-dual Abelian gauge fields,  $\tilde{F}F = \pm F^2$ . On the domain wall the gluon field is Abelian chromomagnetic with vanishing topological charge density  $\tilde{F}F = 0$  and value of the scalar invariant  $F^2 = B_{\text{vac}}^2$  being the same as in the bulk of the domains. Group theoretical analysis of the Weyl symmetry and  $SU(N_c)$  subgroup embeddings behind the domain wall formation in the effective gauge theories, including the present Ginzburg-Landau approach, was given in paper [20].

In recent paper [33] the approach outlined in articles [6, 18, 9, 24] has been considerably evolved in two respects: explicit analytical construction of the domain wall network in  $R^4$  through a combination of additive and multiplicative superpositions of kinks, and refining the spectrum and eigenmodes of the color charged scalar, spinor and vector fields in the background of a domain wall. In particular the spectrum of quasiparticles inside the thick domain wall junction was evaluated indicating existence of the critical size  $L_c \approx 1 fm$  for the stable junction.

## 2. Nonzero gluon condensate $\langle g^2 F^2 \rangle$ and domain wall network as QCD vacuum

The functional renormalization group RG result [19] supported conclusions of [6, 18] based on the Ginzburg-Landau type effective Lagrangian of the form

$$\begin{aligned} \mathcal{L}_{\text{eff}} &= -\frac{1}{4\Lambda^2} \left( D_{\nu}^{ab} F_{\rho\mu}^b D_{\nu}^{ac} F_{\rho\mu}^c + D_{\mu}^{ab} F_{\mu\nu}^b D_{\rho}^{ac} F_{\rho\nu}^c \right) - U_{\text{eff}} \\ U_{\text{eff}} &= \frac{\Lambda^4}{12} \text{Tr} \left( C_1 \check{f}^2 + \frac{4}{3} C_2 \check{f}^4 - \frac{16}{9} C_3 \check{f}^6 \right), \end{aligned} \quad (2.1)$$

where  $\Lambda$  is a scale of QCD related to gluon condensate,  $\check{f} = \tilde{F}/\Lambda^2$ , and

$$\begin{aligned} D_{\mu}^{ab} &= \delta^{ab} \partial_{\mu} - i\check{A}_{\mu}^{ab} = \partial_{\mu} - iA_{\mu}^c (T^c)^{ab}, \\ F_{\mu\nu}^a &= \partial_{\mu} A_{\nu}^a - \partial_{\nu} A_{\mu}^a - if^{abc} A_{\mu}^b A_{\nu}^c, \\ \check{F}_{\mu\nu} &= F_{\mu\nu}^a T^a, \quad T_{bc}^a = -if^{abc} \\ \text{Tr}(\check{F}^2) &= \check{F}_{\mu\nu}^{ab} \check{F}_{\nu\mu}^{ba} = -3F_{\mu\nu}^a F_{\mu\nu}^a \leq 0, \\ C_1 > 0, C_2 > 0, C_3 > 0. \end{aligned}$$

The idea behind (2.1) is the following. One assumes (knows from the hadron phenomenology, e.g. QCD sum rules) that there is nonzero scalar gluon condensate  $\langle g^2 F^2 \rangle$ . This condensate exists due to the quantum effects. One constructs a minimal form of the invariant with respect to all relevant QCD symmetry transformations effective potential with nonzero condensate at the minimum. Naturally, it is assumed that UV renormalization is implemented and (if quarks are present) the massless quark limit is regular. We stress that at this point nothing has been assumed about the particular character of the gauge field potential  $A_{\mu}^a$ . Given the form of effective potential one

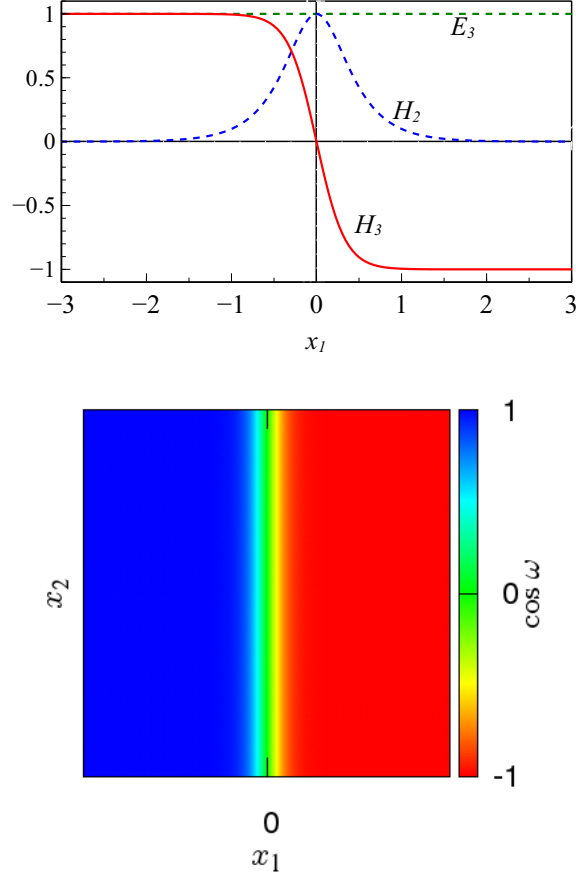


**Figure 1:** Kink profile in terms of the components of the chromomagnetic and chromoelectric field strengths (upper plot), and a two-dimensional slice for the topological charge density in the presence of a single kink measured in units of  $g^2 F_{\alpha\beta}^b F_{\alpha\beta}^b$  (lower plot) that stays constant everywhere. Here  $\omega$  is the angle between the chromomagnetic and chromoelectric fields,  $\cos \omega = F_{\mu\nu}^a \tilde{F}_{\mu\nu}^a / F_{\alpha\beta}^b F_{\alpha\beta}^b$ . The three-dimensional planar domain wall separates the four-dimensional regions filled with the self-dual (blue color) and anti-self-dual (red color) Abelian covariantly constant gluon fields. The chromomagnetic and chromoelectric fields are orthogonal to each other inside the wall (green color).

has to study the various gauge fields with a constant strength. Covariantly constant Abelian (anti-)self-dual gauge fields can be identified as the minimum of the potential. After that one looks for space-time dependent deformations of the field adding the simplest terms with the covariant derivatives. At this step effective equations of motion have to be considered and lead to the domain wall configurations. A comprehensive group theoretical analysis of the symmetries of above effective potential can be found in [20].

The basic input is the existence of the nonzero gluon condensate. An output is somewhat unexpected – existence of twelve (for  $SU(3)$ ) global degenerate discrete minima. The minima are achieved for covariantly constant Abelian (anti-)self-dual fields

$$\check{A}_\mu = -\frac{1}{2} \check{n}_k F_{\mu\nu} x_\nu, \quad \tilde{F}_{\mu\nu} = \pm F_{\mu\nu},$$

where the matrix  $\check{n}_k$  belongs to the Cartan subalgebra of  $su(3)$

$$\begin{aligned}\check{n}_k &= T^3 \cos(\xi_k) + T^8 \sin(\xi_k), \\ \xi_k &= \frac{2k+1}{6}\pi, k = 0, 1, \dots, 5.\end{aligned}\quad (2.2)$$

The values  $\xi_k$  correspond to the boundaries of the Weyl chambers in the root space of  $su(3)$ . The minima are connected by the discrete parity and Weyl transformations, which indicates that the system is prone to existence of solitons (in real space-time) and kink configurations (in Euclidean space). Below we shall concentrate on the simplest configuration – kink interpolating between self-dual and anti-self-dual Abelian vacua. If the angle  $\omega$  between chromoelectric and chromomagnetic fields is allowed to deviate from the constant vacuum value and all other parameters are fixed to the vacuum values, then the Lagrangian takes the form

$$\mathcal{L}_{\text{eff}} = -\frac{1}{2}\Lambda^2 b_{\text{vac}}^2 \partial_\mu \omega \partial_\mu \omega - b_{\text{vac}}^4 \Lambda^4 (C_2 + 3C_3 b_{\text{vac}}^2) \sin^2 \omega,$$

with the corresponding sine-Gordon equation

$$\partial^2 \omega = m_\omega^2 \sin 2\omega, \quad m_\omega^2 = b_{\text{vac}}^2 \Lambda^2 (C_2 + 3C_3 b_{\text{vac}}^2),$$

and the standard kink solution

$$\omega(x_\mu) = 2 \arctg(\exp(\mu x_\mu)) \quad (2.3)$$

interpolating between 0 and  $\pi$ . Here  $x_\mu$  stays for one of the four Euclidean coordinates. The kink describes a planar domain wall between the regions with almost homogeneous Abelian self-dual and anti-self-dual gluon fields. Chromomagnetic and chromoelectric fields are orthogonal to each other on the wall, see Fig.1. Far from the wall, the topological charge density is constant, its absolute value is equal to the value of the gluon condensate. The topological charge density vanishes on the wall. The upper plot shows the profiles of the components of the chromomagnetic and chromoelectric fields corresponding to the Bloch domain wall – the chromomagnetic field flips in the direction parallel to the wall plane.

The domain wall network can be now constructed by the standard methods [25]. The general kink configuration can be parametrized as

$$\zeta(\mu_i, \eta_v^i x_v - q^i) = \frac{2}{\pi} \arctan \exp(\mu_i (\eta_v^i x_v - q^i)),$$

where  $\mu_i$  is the inverse width of the kink,  $\eta_v^i$  is a normal vector to the plane of the wall,  $q^i = \eta_v^i x_v^i$  with  $x_v^i$  - coordinates of the wall.

For an appropriate choice of normal vectors  $\eta^i$  the product

$$\omega(x) = \pi \prod_{i=1}^k \zeta(\mu_i, \eta_v^i x_v - q^i). \quad (2.4)$$

represents a lump of anti-self-dual field in the background of the self-dual one, in two, three and four dimensions for  $k = 4, 6, 8$ , respectively. The general kink network is then given by the additive superposition of lumps (2.4)

$$\omega = \pi \sum_{j=1}^{\infty} \prod_{i=1}^k \zeta(\mu_{ij}, \eta_v^{ij} x_v - q^{ij}). \quad (2.5)$$

The corresponding topological charge densities for different values of the width parameters  $\mu_i$  are shown in Fig. 2. The most LHS plot of Fig. 2 represents the configuration with infinitely thin domain wall defects, that is the Abelian homogeneous (anti-)self-dual field almost everywhere in  $R^4$  characterized by the nonzero absolute value of the topological charge density which is constant and proportional to the value of the action density almost everywhere.

The most RHS plot in Fig. 2 shows the opposite case of the network composed of very thick kinks. Green color corresponds to the gauge field with an infinitesimally small topological charge density. Study of the spectrum of colorless and color charged fluctuations [33] indicates that the LHS configuration is expected to be confining (only colorless hadrons can be excited as particles) while the RHS one supports the color charged quasiparticles as the elementary excitations.

It is expected that the RHS configuration can be triggered by external electromagnetic fields [9, 26, 27]. Strong electromagnetic fields emerge in relativistic heavy ion collisions [28, 29, 30]. Even after switching off the external electromagnetic field the nearly pure chromomagnetic vacuum configuration (RHS of Fig.2) can support strong anisotropies [31] and, in particular, influence the chiral symmetry realization in the collision region [32]. A detailed consideration of the spectrum of elementary color charged excitations at the domain wall junctions (the green regions) is given in [33].

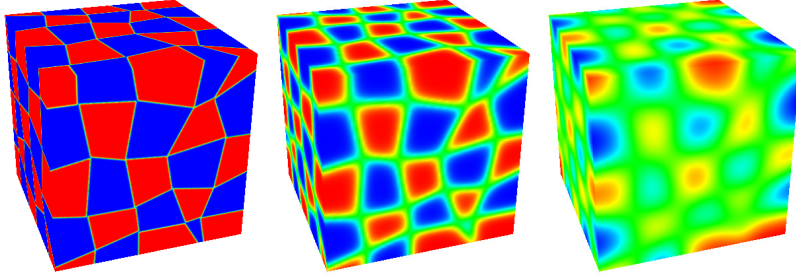


**Figure 2:** Three-dimensional slices of the kink network - additive superposition of numerous four-dimensional lumps. Green color corresponds to the gauge field with infinitesimally small topological charge density.

A comment on representation of the domain wall network in terms of the vector potential is in order. The domain wall network constructed in this section relies on the separation of the Abelian part from the general gauge field. The vector potential representation can be easily realized for the planar Bloch domain wall and layered superposition of planar walls. The same is true also for the interior of a thick domain wall junction, where field is almost homogeneous. The description of the domain walls in the general network Fig. 2 in terms of the vector potential requires application of the gauge field parametrization suggested in a series of papers by Y.M. Cho [34, 35], S. Shabanov [36, 37], L.D. Faddeev and A. J. Niemi [38] and, recently, by K.-I. Kondo [39]. In this

parameterization the Abelian part  $\hat{V}_\mu(x)$  of the gauge field  $\hat{A}_\mu(x)$  is separated manifestly,

$$\begin{aligned}\hat{A}_\mu(x) &= \hat{V}_\mu(x) + \hat{X}_\mu(x), \quad \hat{V}_\mu(x) = \hat{B}_\mu(x) + \hat{C}_\mu(x), \\ \hat{B}_\mu(x) &= [n^a A_\mu^a(x)] \hat{n}(x) = B_\mu(x) \hat{n}(x), \\ \hat{C}_\mu(x) &= g^{-1} \partial_\mu \hat{n}(x) \times \hat{n}(x), \\ \hat{X}_\mu(x) &= g^{-1} \hat{n}(x) \times (\partial_\mu \hat{n}(x) + g \hat{A}_\mu(x) \times \hat{n}(x)),\end{aligned}\tag{2.6}$$

where  $\hat{A}_\mu(x) = A_\mu^a(x) t^a$ ,  $\hat{n}(x) = n_a(x) t^a$ ,  $n^a n^a = 1$ , and

$$\partial_\mu \hat{n} \times \hat{n} = i f^{abc} \partial_\mu n^a n^b t^c, \quad [t^a, t^b] = i f^{abc} t^c.$$

The field  $\hat{V}_\mu$  is seen as the Abelian field in the sense that  $[\hat{V}_\mu(x), \hat{V}_\nu(x)] = 0$ . The color vector field  $n^a(x)$  may be used for detailed description of the thin domain wall junctions in general case. One can see that both the color and space orientation of the field can become frustrated at the junction location and, thus, develop the singularities in the vector potential. These singularities can be expected to be pure gauge ones as soon as the gauge invariant quantities stay regular in the limit of infinitely thin domain wall. The singularities may cover the whole range of defects – vortex-like, dyon-like and zero-dimensional instanton-like defects.

### 3. Ensemble properties and the elementary color charged excitations

#### 3.1 Domain bulk

It is known that the presence of a planar domain wall does not destroy confinement in the bulk of domains, as well as interior of the planar domain wall exhibits color charged quasiparticles [33]. The details of statistical properties of the domain ensemble in its present formulation have yet to be investigated. However, its main properties can be foreseen due to the detailed study of the simplified version of the domain ensemble with spherical domains performed in [6, 24, 8]. The study indicated that the ensemble provides one with both static (area law) and dynamical (purely discrete spectrum of color charged excitations, there are no poles in their propagators), spontaneously broken flavour chiral symmetry,  $U_A(1)$  being broken due to the axial anomaly, absence of the strong CP violation.

Though these studies have given an overall coherent system of guidelines for description of confinement, chiral symmetry realisation, hadronization (see below), it has been always completely unclear what are the mechanisms for deconfinement and chiral symmetry restoration within the framework of the present approach.

More detailed construction of the domain ensemble allows one to recover certain physical mechanisms for deconfinement. The gluon field inside the thick domain wall junction is purely chromomagnetic and allows the color charged quasi-particles. Confinement is lost inside the junction of a finite size. The domain wall junction plays the role of a trap for charged quasi-particles. There exists a critical size of the stable trap, beyond which the emerging tachyonic Nielsen-Olesen gluon modes destroy it.

The chromomagnetic traps as well as any domain wall or junction can be treated as seeds of deconfinement phase randomly distributed in the phase with confinement. At zero mean energy

density and baryon density, in the absence of strong electromagnetic fields and other relevant external influence, i.e. at normal conditions, the deconfinement phase occupies a statistically negligible fraction of the total space-time volume of the system. Under extreme conditions the fraction of deconfinement phase may grow and become statistically dominant.

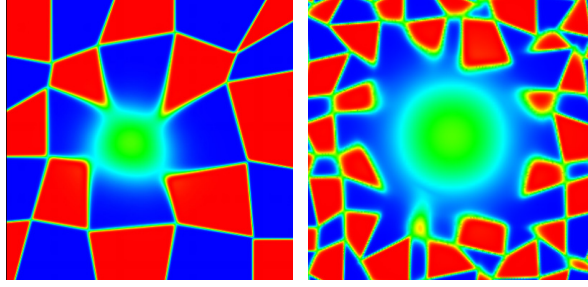


**Figure 3:** Examples of two-dimensional slice of the cylindrical thick domain wall junctions. Blue and red regions represent self-dual and anti-self-dual lumps. Confinement is lost in the green region where  $g^2 \tilde{F}_{\mu\nu}(x)F_{\mu\nu}(x) = 0$ . The scalar condensate density  $g^2 \tilde{F}_{\mu\nu}(x)F_{\mu\nu}(x)$  is nonzero and homogeneous everywhere.

### 3.2 The spectrum of color charged quasiparticles trapped in a thick domain wall junction

For illustration of above statement it is appropriate to consider the eigenmodes of color charged fields inside the cylindrical domain wall junction. One has to solve the Minkowski space Klein-Gordon and Dirac equations in the presence of chromomagnetic field inside the cylinder with the bag-like boundary conditions [33]. Solutions describe the elementary quasiparticle excitations inside the junction. Quite detailed analysis of the notion of quasiparticles in relativistic quantum field theory can be found in [51]. In generic relativistic frame both chromoelectric and chromomagnetic fields are present inside the domain wall junction. However since the topological charge density vanishes in the region (see Fig.3) there exists specific frame where chromoelectric field is absent. This frame is the most convenient for our purposes.

**Adjoint representation: color charged bosons** In the adjoint representation the elementary scalar field excitations  $\phi^a$  inside the cylindrical trap are given by a complex scalar field

$$\phi^a(x) = \sum_{lk} \int_{-\infty}^{+\infty} \frac{dp_3}{2\pi} \frac{1}{\sqrt{2\omega_{alk}}} [a_{akl}^+(p_3) e^{ix_0\omega_{akl} - ip_3x_3} + b_{akl}(p_3) e^{-ix_0\omega_{akl} + ip_3x_3}] e^{il\vartheta} \phi_{alk}(r), \quad (3.1)$$

$$\phi^{a\dagger}(x) = \sum_{lk} \int_{-\infty}^{+\infty} \frac{dp_3}{2\pi} \frac{1}{\sqrt{2\omega_{alk}}} [b_{akl}^+(p_3) e^{-ix_0\omega_{akl} + ip_3x_3} + a_{akl}(p_3) e^{ix_0\omega_{akl} - ip_3x_3}] e^{-il\vartheta} \phi_{alk}(r),$$

$$p_0^2 = p_3^2 + \mu_{akl}^2,$$

$$p_0 = \pm \omega_{akl}(p_3), \quad \omega_{akl} = \sqrt{p_3^2 + \mu_{akl}^2}, \quad (3.2)$$

$$k = 0, 1, \dots, \infty, \quad l \in Z,$$

with  $\phi_{alk}(r)$  normalized as

$$\int_0^\infty dr r \int_0^{2\pi} d\vartheta e^{i(l-l')\vartheta} \phi_{alk}(r) \phi_{al'k'}(r) = \delta_{ll'} \delta_{kk'}.$$

Explicit analytical form of  $\phi_{alk}(r)$  expressed in terms of confluent hypergeometric functions can be found in [33].

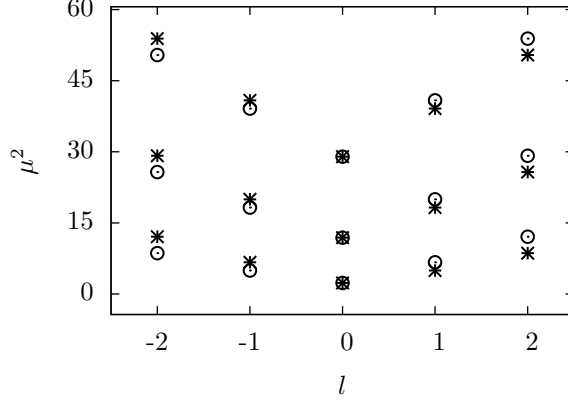


**Figure 4:** Quasiparticle masses squared  $\mu_{alk}^2$  for the scalar field problem,  $l = -2, -1, 0, 1, 2$  and  $k = 0, 1, 2$ , for  $\sqrt{HR} = 1.6$ , in units of chromomagnetic field strength  $H$ . Asterisks (circles) correspond to positive (negative) eigenvalues of the adjoint color matrix  $\check{n}$ .

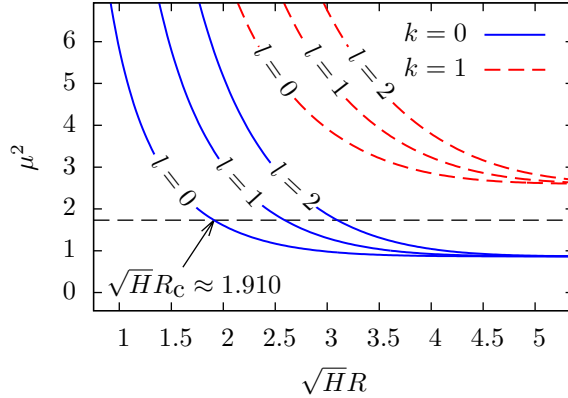


**Figure 5:** The mass squared of the lowest eigenmodes (in units of  $H$ ) as functions of  $\sqrt{HR}$ . The critical radius  $R_c$  corresponds to  $\mu_{a00}^2 = \sqrt{3}H$ . For large  $\sqrt{HR}$  eigenvalues approach correct Landau levels, the degeneracy in  $l$  is restored.

Equation (3.2) can be treated as the dispersion relation between energy  $p_0$  and momentum  $p_3$  for the quasiparticles with masses  $\mu_{akl}$ . These quasiparticles are extended in  $x_1$  and  $x_2$  directions and are classified by the quantum numbers  $l, k$ . The orthogonality, normalization and completeness of the set of functions  $e^{il\vartheta} \phi_{alk}(r)$  guarantees the standard canonical commutation relations for the field  $\phi^a$  and its canonically conjugated momentum if  $a_{akl}^\dagger(p_3)$ ,  $a_{akl}(p_3)$ ,  $b_{akl}^\dagger(p_3)$  and  $b_{akl}(p_3)$  are assumed to satisfy the standard commutation relations for creation and annihilation operators. The

Fock space of states for the quasiparticles with masses  $\mu_{akl}$  can be constructed by means of the standard QFT methods. This treatment provides one with a suitable terminology and formalism for discussion of the confining properties of various gluon field configurations in the context of QFT: unlike the chromomagnetic field the (anti-)self-dual fields characteristic for the bulk of domain network configuration (see the LHS plot in Fig. 2) lead to purely discrete spectrum of eigenmodes in Euclidean space and do not possess any quasiparticle treatment in terms of dispersion relation between energy and momentum for elementary color charged excitations. If there is a reason for long-lived defect in the form of thick domain wall junction then its boundary defines a shape and a size for the space region which can be populated by color charged quasiparticles.

The vector adjoint field can be elaborated in the similar to the scalar case way. A modification relates just to the inclusion of polarization vectors. The most important feature is the absence of tachyonic mode (Nielsen-Olesen mode) of the vector color charged field if the cylinder radius is sufficiently small  $R < R_c$  (see Fig.5). To estimate the critical size one may use the mean phenomenological value of the gluon condensate (gauge coupling constant  $g$  is included into the field strength tensor)

$$\langle F_{\mu\nu}^a F^{a\mu\nu} \rangle = 2H^2 \approx 0.5 \text{ GeV}^4.$$

One arrives at to the critical radius

$$R_c \approx 0.51 \text{ fm} \quad (2R_c \approx 1 \text{ fm}). \quad (3.3)$$

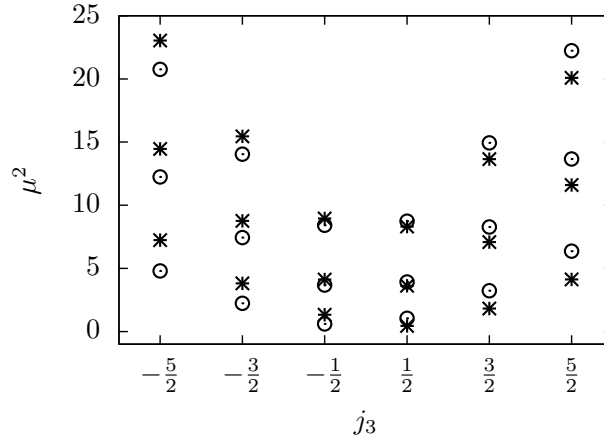


**Figure 6:** The effective masses of fermion quasiparticles  $\mu^2$  for  $\sqrt{HR} = 1.6$ , in units of  $H$ . Here  $j_3 = l + 1/2$  is the projection of the total angular momentum on the direction of the chromomagnetic field. Asterisks (circles) correspond to positive (negative) eigenvalues of the fundamental color matrix  $\hat{n}$ .

**Fundamental representation: color charged fermions** The solution of the Dirac equation

$$i\mathcal{D}\psi(x) = 0,$$

inside the cylindrical trap are characterized by the dispersion relation for the modes with definite projection of the total angular momentum  $j_3$ , radial number  $k$  and color "orientation"  $j$

$$p_0^2 = p_3^2 + \mu_{jlk}^2, \quad p_0 = \pm \omega_{jlk}(p_3),$$

$$\omega_{jlk} = \sqrt{p_3^2 + \mu_{jlk}^2},$$

where  $\mu_{jlk}$  are the effective masses of fermion quasiparticles, see Fig.6.

The solution of the Dirac equation takes the form (for analytical form of  $\Phi(r)$  see [33])

$$\begin{aligned}\psi^j(x) &= \sum_{lk} \int_{-\infty}^{+\infty} \frac{dp_3}{2\pi} \frac{1}{\sqrt{2\omega_{jlk}}} \left[ a_{jlk}^\dagger(p_3) \chi_{jlk}(p_3|r, \vartheta) e^{ix_0\omega_{jlk} - ix_3 p_3} + b_{jlk}(p_3) v_{jlk}(p_3|r, \vartheta) e^{-ix_0\omega_{jlk} + ix_3 p_3} \right], \\ \bar{\psi}^j(x) &= \sum_{lk} \int_{-\infty}^{+\infty} \frac{dp_3}{2\pi} \frac{1}{\sqrt{2\omega_{jlk}}} \left[ b_{jlk}^\dagger(p_3) \bar{\chi}_{jlk}(p_3|r, \vartheta) e^{-ix_0\omega_{jlk} + ix_3 p_3} + a_{jlk}(p_3) \bar{v}_{jlk}(p_3|r, \vartheta) e^{ix_0\omega_{jlk} - ix_3 p_3} \right].\end{aligned}$$

Here the pair of spinors for positive  $\chi_{lk}$  and negative  $v_{lk}$  energy solutions are

$$\chi_{lk} = A_{lk} \begin{pmatrix} (-1)^{k+1} \frac{\mu_{lk}}{\sqrt{\omega_{lk} + p_3}} \Phi_l^{\uparrow\uparrow}(r) e^{il\vartheta} \\ i(-1)^{k+1} \frac{\mu_{lk} \sqrt{\omega_{lk} + p_3}}{2(l+1)} \Phi_{l+1}^{\uparrow\downarrow}(r) e^{i(l+1)\vartheta} \\ i\sqrt{\omega_{lk} + p_3} \Phi_l^{\uparrow\uparrow}(r) e^{il\vartheta} \\ \frac{\mu_{lk}^2}{2(l+1)\sqrt{\omega_{lk} + p_3}} \Phi_{l+1}^{\uparrow\downarrow}(r) e^{i(l+1)\vartheta} \end{pmatrix}, \quad v_{lk} = A_{lk} \begin{pmatrix} (-1)^{k+1} \frac{\mu_{lk}}{\sqrt{\omega_{lk} + p_3}} \Phi_l^{\uparrow\uparrow}(r) e^{il\vartheta} \\ i(-1)^k \frac{\mu_{lk} \sqrt{\omega_{lk} + p_3}}{2(l+1)} \Phi_{l+1}^{\uparrow\downarrow}(r) e^{i(l+1)\vartheta} \\ -i\sqrt{\omega_{lk} + p_3} \Phi_l^{\uparrow\uparrow}(r) e^{il\vartheta} \\ \frac{\mu_{lk}^2}{2(l+1)\sqrt{\omega_{lk} + p_3}} \Phi_{l+1}^{\uparrow\downarrow}(r) e^{i(l+1)\vartheta} \end{pmatrix}$$

for  $l \geq 0$  and

$$\chi_{lk} = B_{lk} \begin{pmatrix} \frac{\mu_{lk}^2}{2l\sqrt{\omega_{lk} + p_3}} \Phi_l^{\uparrow\uparrow}(r) e^{il\vartheta} \\ i\sqrt{\omega_{lk} + p_3} \Phi_{l+1}^{\uparrow\downarrow}(r) e^{i(l+1)\vartheta} \\ i(-1)^k \frac{\mu_{lk} \sqrt{\omega_{lk} + p_3}}{2l} \Phi_l^{\uparrow\uparrow}(r) e^{il\vartheta} \\ (-1)^k \frac{\mu_{lk}}{\sqrt{\omega_{lk} + p_3}} \Phi_{l+1}^{\uparrow\downarrow}(r) e^{i(l+1)\vartheta} \end{pmatrix}, \quad v_{lk} = B_{lk} \begin{pmatrix} \frac{\mu_{lk}^2}{2l\sqrt{\omega_{lk} + p_3}} \Phi_l^{\uparrow\uparrow}(r) e^{il\vartheta} \\ -i\sqrt{\omega_{lk} + p_3} \Phi_{l+1}^{\uparrow\downarrow}(r) e^{i(l+1)\vartheta} \\ i(-1)^{k+1} \frac{\mu_{lk} \sqrt{\omega_{lk} + p_3}}{2l} \Phi_l^{\uparrow\uparrow}(r) e^{il\vartheta} \\ (-1)^k \frac{\mu_{lk}}{\sqrt{\omega_{lk} + p_3}} \Phi_{l+1}^{\uparrow\downarrow}(r) e^{i(l+1)\vartheta} \end{pmatrix}$$

for  $l < 0$ . The spinors are normalized as

$$\int_0^{2\pi} d\vartheta \int_0^R dr r \chi_{jlk}^\dagger(p_3|r, \vartheta) \chi_{jlk}(p_3|r, \vartheta) = \int_0^{2\pi} d\vartheta \int_0^R dr r v_{jlk}^\dagger(p_3|r, \vartheta) v_{jlk}(p_3|r, \vartheta) = 2\omega_{jlk}.$$

The Dirac conjugated spinors are

$$\bar{\psi}^j(x) = \psi^{j\dagger}(x) \gamma_0$$

as usual. The Fock space can be constructed by means of the creation and annihilation operators

$$\left\{ a_{jlk}^\dagger(p_3), a_{jlk}(p_3), b_{jlk}^\dagger(p_3), b_{jlk}(p_3) \right\}$$

satisfying the standard anticommutation relations. The one-particle state is characterized by a color orientation  $j$ , momentum  $p_3$ , projection  $j_3 = (l + 1/2)$  of the total angular momentum and the energy  $\omega_{jlk} = \sqrt{p_3^2 + \mu_{jlk}^2}$ .

#### 4. The strong electromagnetic field as a trigger for deconfinement

It has been observed that the strong electromagnetic fields generated in relativistic heavy ion collisions can play the role of a trigger for deconfinement [9]. The electric  $\mathbf{E}_{el}$  and magnetic  $\mathbf{H}_{el}$  fields are practically orthogonal to each other [29, 28]:  $\mathbf{E}_{el} \mathbf{H}_{el} \approx 0$ . For this configuration of the

$m_{u/d}, \text{MeV}$	$m_s, \text{MeV}$	$m_c, \text{MeV}$	$m_b, \text{MeV}$	$\Lambda, \text{MeV}$	$g$
156	389	1575	4868	418	6.97

**Table 1:** Values of parameters used for calculations of the masses and decay constants given in all other tables

external electromagnetic field the one-loop quark contribution to the QCD effective potential for the homogeneous Abelian gluon fields is minimal for the chromoelectric and chromomagnetic fields directed along the electric and magnetic fields respectively. The orthogonal chromo-fields are not confining: color charged quasiparticles can move along the chromomagnetic field. It has been noted also that this mechanism assumes the strong azimuthal anisotropy in momentum distribution of color charged quasiparticles. Deconfined quarks as well as gluons can move preferably along the direction of the magnetic field but this happens due to the gluon field configuration even after switching the electromagnetic field off.

A detailed and systematic analytical one-loop calculation of the QCD effective potential for the pure chromomagnetic field was performed recently in [41] and confirmed the result that the chromomagnetic field prefers to be parallel (or anti-parallel) to the external magnetic field. Another important source of verification of the basic observations of paper [9] is due to the recent Lattice QCD studies of the response of the QCD vacuum to external electromagnetic fields [26, 27, 42, 43, 44, 45].

In particular, in qualitative agreement with [9] Lattice QCD study [27] has demonstrated that in the presence of external magnetic field the gluonic action develops an anisotropy: the chromomagnetic field parallel to the external field is enhanced, while the chromo-electric field in this direction is suppressed. The results of [42] indicated that the magnetic field can affect the azimuthal structure of the expansion of the system during heavy ion collisions.

Within the context of the confining domain wall network these observations mean that a flash of the strong electromagnetic field during heavy ion collisions produces a kind of defect in the form of the thick domain wall junction in the confining gluon background exactly in the region where collision occurs (see Fig.3). The electromagnetic flash can act as one of the preconditions for conversion of the high energy density and baryon density to the thermodynamics of color charged degrees of freedom.

## 5. Color neutral collective excitations

In this section we present the new results of calculation of the spectrum of radial meson excitations within the framework of domain model. Ground state and orbital excitations of light, heavy-light mesons and heavy quarkonia were considered in [22, 23, 24]. In these previous calculations the non-diagonal in radial quantum number terms in the effective meson action were neglected. Here we improve the calculation in this respect. Technical details and approximations of the bosonization procedure in application to the partition function (1.2) can be found in papers [22, 23, 24].

### 5.1 Effective meson action

The quantum field dynamics of collective boson modes in the domain ensemble is described by the Euclidean functional integral [24]

$$Z = \mathcal{N} \lim_{V \rightarrow \infty} \int D\Phi_{\mathcal{Q}} \exp \left\{ -\frac{B}{2} \frac{h_{\mathcal{Q}}^2}{g^2 C_{\mathcal{Q}}} \int dx \Phi_{\mathcal{Q}}^2(x) - \sum_k \frac{1}{k} W_k[\Phi] \right\}, \quad (5.1)$$

$$1 = \frac{g^2 C_{\mathcal{Q}}}{B} \tilde{\Gamma}_{\mathcal{Q}\mathcal{Q}}^{(2)}(-M_{\mathcal{Q}}^2|B), \quad (5.2)$$

$$h_{\mathcal{Q}}^{-2} = \frac{d}{dp^2} \tilde{\Gamma}_{\mathcal{Q}\mathcal{Q}}^{(2)}(p^2)|_{p^2=-M_{\mathcal{Q}}^2}. \quad (5.3)$$

The effective action in Eq. (5.1) is expressed in terms of colourless composite meson fields  $\Phi_{\mathcal{Q}}(x)$  with the mass  $M_{\mathcal{Q}}$  defined by Eq. (5.2), where the condensed index  $\mathcal{Q}$  denotes isotopic and space-time indices as well as all possible mesonic quantum numbers (iso-spin, spin-parity in the ground state, total momentum, radial quantum number), and  $k$ -point nonlocal vertices  $\Gamma_{\mathcal{Q}_1 \dots \mathcal{Q}_k}^{(k)}$

$$W_k[\Phi] = \sum_{\mathcal{Q}_1 \dots \mathcal{Q}_k} h_{\mathcal{Q}_1} \dots h_{\mathcal{Q}_k} \int dx_1 \dots \int dx_k \Phi_{\mathcal{Q}_1}(x_1) \dots \Phi_{\mathcal{Q}_k}(x_k) \Gamma_{\mathcal{Q}_1 \dots \mathcal{Q}_k}^{(k)}(x_1, \dots, x_k|B),$$

$$\Gamma_{\mathcal{Q}_1}^{(1)} = \overline{G_{\mathcal{Q}_1}^{(1)}}, \quad (5.4)$$

$$\Gamma_{\mathcal{Q}_1 \mathcal{Q}_2}^{(2)} = \overline{G_{\mathcal{Q}_1 \mathcal{Q}_2}^{(2)}(x_1, x_2) - \Xi_2(x_1 - x_2) \overline{G_{\mathcal{Q}_1}^{(1)} G_{\mathcal{Q}_2}^{(1)}}}, \quad (5.5)$$

$$\Gamma_{\mathcal{Q}_1 \mathcal{Q}_2 \mathcal{Q}_3}^{(3)} = \overline{G_{\mathcal{Q}_1 \mathcal{Q}_2 \mathcal{Q}_3}^{(3)}(x_1, x_2, x_3) - \frac{3}{2} \Xi_2(x_1 - x_3) \overline{G_{\mathcal{Q}_1 \mathcal{Q}_2}^{(2)}(x_1, x_2) G_{\mathcal{Q}_3}^{(1)}(x_3)} + \frac{1}{2} \Xi_3(x_1, x_2, x_3) \overline{G_{\mathcal{Q}_1}^{(1)}(x_1) G_{\mathcal{Q}_2}^{(1)}(x_2) G_{\mathcal{Q}_3}^{(1)}(x_3)}}, \quad (5.6)$$

$$\Gamma_{\mathcal{Q}_1 \mathcal{Q}_2 \mathcal{Q}_3 \mathcal{Q}_4}^{(4)} = \overline{G_{\mathcal{Q}_1 \mathcal{Q}_2 \mathcal{Q}_3 \mathcal{Q}_4}^{(4)}(x_1, x_2, x_3, x_4) - \frac{4}{3} \Xi_2(x_1 - x_2) \overline{G_{\mathcal{Q}_1}^{(1)}(x_1) G_{\mathcal{Q}_2 \mathcal{Q}_3 \mathcal{Q}_4}^{(3)}(x_2, x_3, x_4)} - \frac{1}{2} \Xi_2(x_1 - x_3) \overline{G_{\mathcal{Q}_1 \mathcal{Q}_2}^{(2)}(x_1, x_2) G_{\mathcal{Q}_3 \mathcal{Q}_4}^{(2)}(x_3, x_4)} + \Xi_3(x_1, x_2, x_3) \overline{G_{\mathcal{Q}_1}^{(1)}(x_1) G_{\mathcal{Q}_2}^{(1)}(x_2) G_{\mathcal{Q}_3 \mathcal{Q}_4}^{(2)}(x_3, x_4)} - \frac{1}{6} \Xi_4(x_1, x_2, x_3, x_4) \overline{G_{\mathcal{Q}_1}^{(1)}(x_1) G_{\mathcal{Q}_2}^{(1)}(x_2) G_{\mathcal{Q}_3}^{(1)}(x_3) G_{\mathcal{Q}_4}^{(1)}(x_4)}}, \quad (5.7)$$

and analogous expressions for the higher vertices. Defining the meson-quark coupling constants  $h_{\mathcal{Q}}$  by Eq. (5.3) provides for the correct residue of the meson propagators at the poles and is known as a compositeness condition.

The meson-meson vertices  $\Gamma^{(k)}$  are expressed *via* quark loops  $G_{\mathcal{Q}}^{(n)}$  with  $n$  quark-meson vertices

$$\overline{G_{\mathcal{Q}_1 \dots \mathcal{Q}_k}^{(k)}(x_1, \dots, x_k)} = \int_{\Sigma} d\sigma_j \text{Tr} V_{\mathcal{Q}_1}(x_1|B^{(j)}) S(x_1, x_2|B^{(j)}) \dots V_{\mathcal{Q}_k}(x_k|B^{(j)}) S(x_k, x_1|B^{(j)})$$

$$\overline{G_{\mathcal{Q}_1 \dots \mathcal{Q}_l}^{(l)}(x_1, \dots, x_l) G_{\mathcal{Q}_{l+1} \dots \mathcal{Q}_k}^{(k)}(x_{l+1}, \dots, x_k)} = \int_{\Sigma} d\sigma_j$$

$$\times \text{Tr} \left\{ V_{\mathcal{Q}_1}(x_1|B^{(j)}) S(x_1, x_2|B^{(j)}) \dots V_{\mathcal{Q}_k}(x_l|B^{(j)}) S(x_l, x_1|B^{(j)}) \right\}$$

$$\times \text{Tr} \left\{ V_{\mathcal{Q}_{l+1}}(x_{l+1}|B^{(j)}) S(x_{l+1}, x_{l+2}|B^{(j)}) \dots V_{\mathcal{Q}_k}(x_k|B^{(j)}) S(x_k, x_{l+1}|B^{(j)}) \right\}, \quad (5.8)$$

meson	n	$M$ , MeV	$M$ , MeV	h
$\pi$	0	139.57 [46]	139.5	3.74
$\pi(1300)$	1	1300 [46]	1364.243	2.46
$K$	0	493.68 [46]	494.0	4.24
$K(1460)$	1	1460 [46]	1380	2.10
$\rho$	0	770 [46]	770	1.97
$\rho(1450)$	1	1450 [46]	1577	1.53
$\rho$	2	1720 [46]	1663	1.57
$K^*$	0	891.7 [46]	892	2.15
$K^*(1410)$	1	1410 [46]	1517	1.52
$\phi$	0	1019.46 [46]	1041	2.40
$\phi(1680)$	1	1680 [46]	1718	1.66
$\phi$	2	2175 [46]	1931	1.58
$D$	0	1864.86 [46]	1712	6.16
$D$	1	2579 [48]	2337	2.69
$D_s$	0	1968.5 [46]	1830	7.08
$D_s$	1	2670 [48]	2604	2.71
$B$	0	5279 [46]	5018	9.62
$B$	1	5883 [48]	5578	4.07
$B_s$	0	5366.7 [46]	5118	11.07
$B_s$	1	5971 [48]	5806	4.02
$B_c$	0	6277 [46]	5981	14.65
$B_c$	1	6842 [49]	6986	4.39
$\eta_c(1S)$	0	2981 [46]	2781	9.84
$\eta_c(2S)$	1	3639 [46]	3620	3.42
$D^*$	0	2010.28 [46]	1944	3.18
$D^*$	1	2629 [48]	2402	1.89
$D_s^*$	0	2112.3 [46]	2092	3.57
$D_s^*$	1	2716 [48]	2659	1.92
$J/\psi(1S)$	0	3096.92 [46]	3097	5.13
$\psi(2S)$	1	3686 [46]	3705	2.32
$\psi(4040)$	2	4039 [46]	3931	2.44
$B^*$	0	5325 [46]	5197	5.20
$B^*$	1	5898 [48]	5620	2.82
$B_s^*$	0	5415.4 [46]	5336	5.80
$B_s^*$	1	5984 [48]	5844	2.80
$\Upsilon(1S)$	0	9460 [46]	9460	10.51
$\Upsilon(2S)$	1	10023 [46]	10109	4.08
$\Upsilon(3S)$	2	10355 [46]	10337	3.68

**Table 2:** The masses and decay constants of ground state and radially excited mesons. Our result is given in the fourth column. The table includes light and heavy-light mesons as well as the heavy quarkonia. Overall accuracy is less than 11%.

where bar denotes integration with measure  $d\sigma_j$  over all configurations of the background domain structured field  $B^{(j)}$ . The form of the nonlocal quark-meson vertex operator  $V_\mu^{ak}(x)$

$$V_{\mu_1 \dots \mu_l}^{aJln}(x) = M^a \Gamma^J \left\{ \left\{ F_{nl} \left( \frac{\overleftrightarrow{\nabla}^2(x)}{\Lambda^2} \right) T_{\mu_1 \dots \mu_l}^{(l)} \left( \frac{1}{i} \frac{\overleftrightarrow{\nabla}^2(x)}{\Lambda^2} \right) \right\} \right\}, \quad (5.9)$$

$$F_{nl}(s) = s^n \int_0^1 dt t^{n+l} \exp(st), \quad (5.10)$$

$$\overleftrightarrow{\nabla} = \overleftarrow{\nabla} \xi_{f'} - \overrightarrow{\nabla} \xi_f, \quad \xi_f = \frac{m_f}{m_f + m_{f'}}, \quad (5.11)$$

$$\overleftarrow{\nabla} = \overleftarrow{\partial}_\mu + i\widehat{B}_\mu(x), \quad \overrightarrow{\nabla} = \overrightarrow{\partial}_\mu - i\widehat{B}_\mu(x). \quad (5.12)$$

is completely determined by the form of the gluon propagator in the presence of the background field.

The quark propagator  $S(x, y)$  in the presence of Abelian (anti-)self-dual field (taken here to be constant with random values of its parameter) has the form

$$S(x, y) = \exp\left(-\frac{i}{2} x_\mu \widehat{B}_{\mu\nu} y_\nu\right) H(x - y),$$

$$\begin{aligned} \widetilde{H}_f(p|B) = \frac{1}{2\nu\Lambda^2} \int_0^1 ds e^{(-p^2/2\nu\Lambda^2)s} \left(\frac{1-s}{1+s}\right)^{m_f^2/4\nu\Lambda^2} \left[ p_\alpha \gamma_\alpha \pm is\gamma_5 \gamma_\alpha f_{\alpha\beta} p_\beta + \right. \\ \left. + m_f \left( P_\pm + P_\mp \frac{1+s^2}{1-s^2} - \frac{i}{2} \gamma_\alpha f_{\alpha\beta} \gamma_\beta \frac{s}{1-s^2} \right) \right], \quad (5.13) \end{aligned}$$

$$P_\pm = (1 \pm \gamma_5)/2, \quad f_{\alpha\beta} = \frac{\hat{n}}{2\nu\Lambda^2} B_{\alpha\beta}, \quad \nu = \text{diag}\left(\frac{1}{6}, \frac{1}{6}, \frac{1}{3}\right), \quad (5.14)$$

$$B_{\mu\nu} = -B_{\nu\mu}, \quad \widetilde{B}_{\mu\nu} = \frac{1}{2} \varepsilon_{\mu\nu\alpha\beta} B_{\alpha\beta} = \pm B_{\mu\nu}, \quad \widehat{B}_{\rho\mu} \widehat{B}_{\rho\nu} = 4\nu^2 \Lambda^4 \delta_{\mu\nu}. \quad (5.15)$$

One can see that all elements in the effective mesonic action are defined in analytical form and ready for calculation of meson spectrum, formfactors, etc.

## 5.2 Radial excitations of mesons

Quadratic part of the effective action in the momentum representation reads

$$I_2 = -\frac{1}{2} \int d^4 p \widetilde{\Phi}_\mu^{ak}(-p) \left[ \Lambda^2 \delta_{\mu\mu'} \delta^{ak, a'k'} + G_k G_{k'} \widetilde{\Pi}_{\mu\mu'}^{ak, a'k'}(p) \right] \widetilde{\Phi}_{\mu'}^{a'k'}(p).$$

Here

$$k = (Jln), \quad \mu = (\mu_1 \dots \mu_l), \quad G_k = g \sqrt{C_J \frac{l+1}{2!n!(n+l)!}}.$$

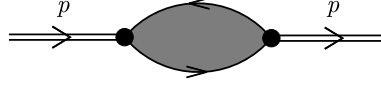


**Figure 7:** One-loop contribution to the polarization function. Light grey color denotes averaging over the background field.

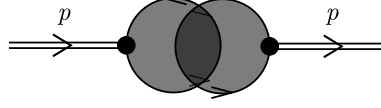


**Figure 8:** Two-loop diagram. Dark grey color indicates the correlated averaging over the background gluon field in two quark loops.

We do not consider here the orbital excitations and put the orbital momentum to be zero  $l = 0$ . The polarization operator  $\Pi^{aJ0n,aJ0n'}(p)$  can be reduced to a rather compact form

$$\begin{aligned} \Pi_J^{nn'}(-M^2; m_f, m_{f'}; \Lambda) = & \\ & -\frac{\Lambda^2}{4\pi^2} \text{Tr}_v \int_0^1 dt_1 \int_0^1 dt_2 \int_0^1 ds_1 \int_0^1 ds_2 \left( \frac{1-s_1}{1+s_1} \right)^{m_f^2/4v\Lambda^2} \left( \frac{1-s_2}{1+s_2} \right)^{m_{f'}^2/4v\Lambda^2} t_1^n t_2^{n'} \frac{\partial^n}{\partial t_1^n} \frac{\partial^{n'}}{\partial t_2^{n'}} \times \\ & \frac{1}{\Phi_2^2} \left[ \frac{M^2}{\Lambda^2} \frac{F_1^{(J)}}{\Phi_2^2} + \frac{m_f m_{f'}}{\Lambda^2} \frac{F_2^{(J)}}{(1-s_1^2)(1-s_2^2)} + \frac{F_3^{(J)}}{\Phi_2} \right] \exp \left\{ \frac{M^2}{2v\Lambda^2} \frac{\Phi_1}{\Phi_2} \right\}. \end{aligned}$$

where

$$\Phi_1 = s_1 s_2 + 2(\xi_1^2 s_1 + \xi_2^2 s_2)(t_1 + t_2)v,$$

$$\Phi_2 = s_1 + s_2 + 2(1 + s_1 s_2)(t_1 + t_2)v + 16(\xi_1^2 s_1 + \xi_2^2 s_2)t_1 t_2 v^2,$$

$$\begin{aligned} F_1^{(P)} = & (1 + s_1 s_2) [2(\xi_1 s_1 + \xi_2 s_2)(t_1 + t_2)v + \\ & 4\xi_1 \xi_2 (1 + s_1 s_2)(t_1 + t_2)^2 v^2 + s_1 s_2 (1 - 16\xi_1 \xi_2 t_1 t_2 v^2)], \end{aligned}$$

$$\begin{aligned} F_1^{(V)} = & \left( 1 - \frac{1}{3}s_1 s_2 \right) [s_1 s_2 + 16\xi_1 \xi_2 t_1 t_2 v^2 + 2(\xi_1 s_1 + \xi_2 s_2)(t_1 + t_2)v] + \\ & 4\xi_1 \xi_2 (1 - s_1^2 s_2^2)(t_1 - t_2)^2 v^2, \end{aligned}$$

$$F_2^{(P)} = (1 + s_1 s_2)^2, \quad F_2^{(V)} = (1 - s_1^2 s_2^2),$$

$$F_3^{(P)} = 4v(1 + s_1 s_2)(1 - 16\xi_1 \xi_2 t_1 t_2 v^2),$$

$$F_3^{(V)} = 2v(1 - s_1 s_2)(1 - 16\xi_1 \xi_2 t_1 t_2 v^2).$$

Diagonalizing of  $\Pi^{aJ0n,aJ0n'}$  with respect to the radial quantum numbers  $n = 0 \dots 3$  and  $n' = 0 \dots 3$  and using (5.3) one arrives at the meson masses listed in the Table 2 for the values of the

meson	n	$M$ , MeV [46]	$M$ , MeV	$h$
$\eta$	0	547.86	499	3.78
$\eta'$	0	957.8	957	3.41
$\eta(1295)$	1	1294	1165	3.08
$\eta(1475)$	1	1476	1366	3.10

**Table 3:** Masses and coupling constants of  $\eta, \eta'$ . For interpretation of the excited states, see [46]. The value of domain radius  $R = 2.374/\Lambda \approx 1.121$  fm is chosen to fit the  $\eta'$  mass. Our result is given in fourth column.

meson	$f_P$ , MeV	$f_P$ , MeV
$K$	156 [46]	159
$\pi$	130 [46]	132
$D$	205 [46]	180
$D_s$	258 [46]	230
$B$	191 [46]	157
$B_s$	253 [47]	205
$B_c$	489 [47]	341

**Table 4:** Decay constants of pseudoscalar mesons.

parameters given in Table 1. Omitting the details we report also the weak decay constants of pseudoscalar mesons, see Table 4.

It should be noted that the masses of all mesons listed in Table 2 are computed by means of the one-loop diagram, Fig. 7. Two-loop contribution, Fig. 8, is irrelevant to these mesons. The situation is completely different in the case of the  $\eta$  and  $\eta'$  (for details see [24]). Taking into account both one- and two-loop contributions in the case of flavour octet and singlet states and diagonalizing the polarization function both in  $(n, n')$  and  $(a = 0, 8; a' = 0, 8)$  we arrive to the masses given in Table 3.

We have to stress here that the model has a minimal set of parameters: scale  $\Lambda$  related to the scalar gluon condensate, quark masses  $m_f$ , gauge coupling constant  $g$  at the scale  $\Lambda$ , and the domain radius  $R$  related to the topological susceptibility of the pure glue vacuum. The domain radius  $R$  was required only for calculation of the  $\eta$  and  $\eta'$  masses. The overall accuracy of description of the masses and decay constant is less than 11%.

## 6. Discussion

Here we would like to discuss further steps that become accessible within the more detailed construction of the domain wall network presented in sections 2 and 3.

Functional integral (1.2) includes integration over the whole statistical ensemble  $\mathcal{B}$ . This infinite dimensional integral can be defined by means of the parametrization of the general kink superposition (2.5) to set up a considerably refined version of the models elaborated in papers [23,

22, 6, 24, 8]. Statistical weight of a given configuration  $B \in \mathcal{B}$  has to be controlled by the QCD effective action emerging from the integral over the fields  $Q$ .

Important observation was that there exists a critical size  $R_c$  of the region (chromomagnetic trap) where deconfined color charged quasiparticles may exist. For overcritical size of the trap the tachyonic gluon modes emerge in the excitation spectrum and destabilize it.

This certainly does not mean that the overall volume of deconfinement transition in hadronic matter is somehow restricted by  $R_c$ . Numerous traps may be formed, the traps may merge into a large purely chromomagnetic lump developing the "spaghetti" flux tube structure inside the lump. Equivalently one may also think about formation of the spaghetti configuration inside the traps with overcritical size emerging under conditions of high energy or/and baryon number density, strong electromagnetic fields.

Unlike the previous formulations the new one allows, at least in principle, to study the deconfinement transition. The general idea of the study can be related to the treatment of heterophase mixed states in condensed matter [52]. As it has already been mentioned in the Introduction, domain walls and their junctions can be treated as representing the seeds of the deconfinement phase randomly distributed in the confinement phase. In the absence of any external impact one expects that the fraction of the deconfinement phase is statistically negligible as it occupies an essentially three-dimensional sub-manifold in the four-dimensional space  $R^4$ .

The domain wall network representation of QCD vacuum is suggestive of a two-stage deconfinement transition. At the first stage topological charge density vanishes but the scalar condensate stays almost unchanged, color charged quasiparticles are activated at this stage while the colorless collective excitations can decay into the color charged ones. At the second stage the scalar gluon condensate vanishes and the system turns into dilute quark-gluon plasma. Detailed consideration requires an additional information about the QCD effective action structure and goes far beyond the scope of the present paper.

## References

- [1] J. Greensite, Lect. Notes Phys. **821** (2011) 1.
- [2] P. Minkowski, Phys. Lett. **B 76** (1978) 439.
- [3] H. Pagels, and E. Tomboulis, Nucl. Phys. B **143** (1978) 485.
- [4] P. Minkowski, Nucl. Phys. B **177** (1981) 203.
- [5] H. Leutwyler, Nucl. Phys. B **179** (1981) 129.
- [6] A.C. Kalloniatis and S.N. Nedelko, Phys. Rev. D **64** (2001) 114025;
- [7] L. D. Faddeev, [arXiv:0911.1013 [math-ph]].
- [8] A.C. Kalloniatis and S.N. Nedelko, Phys. Rev. D **73** (2006) 034006.
- [9] B.V. Galilo and S.N. Nedelko, Phys. Rev. D **84** (2011) 094017.
- [10] N.K. Nielsen, P. Olesen, Phys. Lett. **B 79**, 304 (1978).
- [11] H.B. Nielsen, P. Olesen. Nucl. Phys. **B 160**, 380 (1979).
- [12] J. Ambjorn, N.K. Nielsen, P. Olesen Nucl. Phys. **B 152**, 75 (1979).

- [13] J. Ambjorn, P. Olesen Nucl. Phys. **B 170**, 265 (1980).
- [14] G. K. Savvidy, Phys. Lett. **B 71** (1977) 133.
- [15] S. G. Matinyan and G. K. Savvidy, Nucl. Phys. **B 134** (1978) 539.
- [16] P. Olesen, Nucl. Phys. **B 200**, 381 (1982).
- [17] H. D. Trottier and R. M. Woloshyn, Phys. Rev. Lett. **70**, 2053 (1993).
- [18] B.V. Galilo and S.N. Nedelko, Phys. Part. Nucl. Lett., **8** (2011) 67 [arXiv:hep-ph/1006.0248v2].
- [19] A. Eichhorn, H. Gies and J. M. Pawłowski, Phys. Rev. **D 83**, 045014 (2011) [Erratum-ibid. **D 83**, 069903 (2011)] [arXiv:1010.2153 [hep-ph]].
- [20] D. P. George, A. Ram, J. E. Thompson and R. R. Volkas, Phys. Rev. **D 87**, 105009 (2013) [arXiv:1203.1048 [hep-th]].
- [21] H. Leutwyler, Phys. Lett. **B 96** (1980) 154.
- [22] G.V. Efimov, and S.N. Nedelko, Phys. Rev. **D 51** (1995) 176;
- [23] J. .V. Burdanov, G. V. Efimov, S. N. Nedelko, S. A. Solunin, Phys. Rev. **D 54** (1996) 4483.
- [24] A.C. Kalloniatis and S.N. Nedelko, Phys. Rev. **D 69** (2004) 074029; *Erratum-ibid.* Phys. Rev. **D 70** (2004) 119903; *ibid.* Phys. Rev. **D 71** (2005) 054002;
- [25] T. Vachaspati, Kinks and Domain Walls, Cambridge University Press, 2006.
- [26] M. D’Elia, M. Mariti and F. Negro, Phys. Rev. Lett. **110**, 082002 (2013) [arXiv:1209.0722 [hep-lat]].
- [27] G. S. Bali, F. Bruckmann, G. Endrodi, F. Gruber and A. Schaefer, JHEP **1304**, 130 (2013) [arXiv:1303.1328 [hep-lat]].
- [28] V. Skokov, A. Y. Illarionov and V. Toneev, Int. J. Mod. Phys. **A 24** (2009) 5925 [arXiv:0907.1396 [nucl-th]].
- [29] V. Voronyuk, V. D. Toneev, W. Cassing, E. L. Bratkovskaya, V. P. Konchakovski and S. A. Voloshin, Phys. Rev. **C 83**, 054911 (2011) [arXiv:1103.4239 [nucl-th]].
- [30] D. E. Kharzeev, L. D. McLerran, and H. J. Warringa, Nucl. Phys. **A 803 227** (2008)
- [31] K. Tuchin, Adv. High Energy Phys. **2013**, 490495 (2013) [arXiv:1301.0099].
- [32] K. Fukushima and Y. Hidaka, Phys. Rev. Lett. **110**, 031601 (2013) [arXiv:1209.1319 [hep-ph]].
- [33] S. N. Nedelko and V. E. Voronin, arXiv:1403.0415 [hep-ph].
- [34] Y.M. Cho, Phys. Rev. Lett. **44** (1980) 1115.
- [35] Y. M. Cho, J. H. Kim and D. G. Pak Mod. Phys. Lett. **A 21** (2006) 2789.
- [36] S.V. Shabanov, J. Math. Phys. **43** (2002) 4127 [hep-th/0202146].
- [37] S. V. Shabanov Phys. Rept. **326** (2000) 1 [arXiv:hep-th/0002043]; S. V. Shabanov and J. R. Klauder Phys. Lett. **B 456** (1999) 38. *L. V. Prokhorov Yad. Fiz.*, **35** (1982) 229.
- [38] L. D. Faddeev, A. J. Niemi, Nucl. Phys. **B. 776**. 2007; *ibid.* Phys. Lett. **B 449**, 214(1999) .
- [39] Kei-Ichi Kondo, Toru Shinohara, Takeharu Murakami, Prog. Theor. Phys. **120** (2008) 1 [arXiv:0803.0176 [hep-th]].
- [40] N. K. Nielsen and P. Olesen, Nucl. Phys. **B 144**, 376 (1978).

- [41] S. Ozaki, Phys. Rev. D **89** (2014) 5, 054022 [arXiv:1311.3137 [hep-ph]].
- [42] G. S. Bali, F. Bruckmann, G. Endrodi and A. Schafer, arXiv:1311.2559 [hep-lat].
- [43] C. Bonati, M. D'Elia, M. Mariti, F. Negro and F. Sanfilippo, arXiv:1312.5070 [hep-lat]; *ibid* Phys. Rev. Lett. **111**, 182001 (2013) [arXiv:1307.8063 [hep-lat]].
- [44] C. Bonati, M. D'Elia, M. Mariti, F. Negro and F. Sanfilippo, Phys. Rev. D **89**, 054506 (2014) [arXiv:1310.8656 [hep-lat]].
- [45] M.D'Elia, M.Mariti, M.Mesiti, F.Negro and F. Sanfilippo, Phys. Rev. D **89**, 114502 (2014) [arXiv:1403.6094 [hep-lat]].
- [46] K.A. Olive et al. ( Particle Data Group) *Chinese Phys. C* **38**,090001, 2014.
- [47] T. W. Chiu *et al.* [TWQCD Collaboration], PoS LAT **2006**, 180 (2007) [arXiv:0704.3495 [hep-lat]].
- [48] D. Ebert, V. O. Galkin and R. N. Faustov, Phys. Rev. D **57**, 5663 (1998) [Erratum-*ibid.* D **59**, 019902 (1999)] [hep-ph/9712318].
- [49] D. Ebert, R. N. Faustov and V. O. Galkin, Eur. Phys. J. C **71**, 1825 (2011) [arXiv:1111.0454 [hep-ph]].
- [50] M. Abramowitz, I.A. Stegun, Handbook of Mathematical Functions with Formulas, Graphs, and Mathematical Tables , Dover (1964), New York .
- [51] D. Arteaga, Annals Phys. **324**, 920 (2009) [arXiv:0801.4324 [hep-ph]].
- [52] V.I. Yukalov, Phys. Rep. **208** (1991) 395; V.I. Yukalov, Int. J. Mod. Phys. B **17**, (2003) 2333; V. I. Yukalov and E. P. Yukalova, PoS ISHEPP **2012**, 046 (2012) [arXiv:1301.6910 [hep-ph]].